





Article

Identification of the Physical and Mechanical Properties of Moroccan Sisal Yarns Used as Reinforcements for Composite Materials

Zineb Samouh ^{1,2,3,*} , Omar Cherkaoui ³, Damien Soulat ¹ , Ahmad Rashed Labanieh ¹ , François Boussu ¹ 
and Reddad El moznine ²

- ¹ GEMTEX Laboratory, ENSAIT, University Lille North of France, F-59100 Roubaix, France; damien.soulat@ensait.fr (D.S.); ahmad.labanieh@ensait.fr (A.R.L.); francois.boussu@ensait.fr (F.B.)
² LPMC Laboratory, Faculty of Science El Jadida, Chouaib Doukkali University, 24000 El Jadida, Morocco; elmoznine@yahoo.fr
³ REMTEX Laboratory, ESITH (Higher School of Textile and Clothing Industries), 7731 Casablanca, Morocco; omarcherkaoui61@gmail.com
* Correspondence: zineb.samouh@gmail.com

Abstract: This work aims to investigate the physical and mechanical properties of sisal fiber and yarn of Moroccan origin. The cellulosic and non-cellulosic constituents of the Moroccan sisal fiber were identified by FTIR spectroscopy. The thermal properties were studied by thermogravimetric analysis. The hydrophilicity of the fiber was evaluated by the contact angle. The results show that the sisal fiber has a low thermal stability. The mechanical properties of the fiber analyzed by the Impregnated Fiber Bundle Test (IFBT) method show that the porosity of the impregnated yarns and the twist angle of the yarns influence the elastic modulus of the sisal fiber. The physical and mechanical properties of the manufactured sisal yarns were also characterized and analyzed. The obtained results reveal an interesting potential to use the Moroccan sisal fiber in development of bio-sourced composite materials.

Keywords: sisal fiber; IFBT method; thermal analysis; sisal yarn; chemical composition



Citation: Samouh, Z.; Cherkaoui, O.; Soulat, D.; Labanieh, A.R.; Boussu, F.; moznine, R.E. Identification of the Physical and Mechanical Properties of Moroccan Sisal Yarns Used as Reinforcements for Composite Materials. *Fibers* **2021**, *9*, 13. <https://doi.org/10.3390/fib9020013>

Academic Editor: Vincenzo Fiore
Received: 21 December 2020
Accepted: 27 January 2021
Published: 5 February 2021

Publisher's Note: MDPI stays neutral with regard to jurisdictional claims in published maps and institutional affiliations.



Copyright: © 2021 by the authors. Licensee MDPI, Basel, Switzerland. This article is an open access article distributed under the terms and conditions of the Creative Commons Attribution (CC BY) license (<https://creativecommons.org/licenses/by/4.0/>).

1. Introduction

Composite materials are high-performance materials used in various fields of application such as automotive, aeronautics, construction. Despite the advantages of conventional composites such as mechanical strength, corrosion resistance and design flexibility, the limitations of composites are related to the nature of their petroleum source (non-biodegradability, manufacturing process with high energy consumption . . .) [1–3].

The use of alternative fibers derived from natural resources to synthetic fibers in the manufacture of composite materials reduces the economic and ecological footprint of these materials and meets environmental regulations on industrial activity [4–6]. Natural fibers have become more attractive to the composite materials industry, which has increased the world production of these fibers (an increase of 2 million tons in ten years 2008–2018). The automotive sector remains the largest market for natural fiber reinforced composites [5,6]. The use of natural fibers in the automotive industry not only concerns the environmental aspect but also the economic aspect by reducing production costs and resin consumption [6]. The low density of natural fibers compared to the density of glass fibers allows the development of lightweight vehicles, which causes reduction in CO₂ emissions.

Different works have focused on a comparative study of composite materials based on synthetic and natural fibers [7–10]. However, while the use of natural fibers as a reinforcement has shown important advantages, major problems have been identified that are related to the nature of the fiber structure, such as moisture absorption and variability of mechanical performance and odor release due to the emission of oxygenated Volatile

organic compounds (VOC's). These problems can be solved, respectively, by chemical treatment of the fibers and by the incorporation of non-porous inorganic fillers to trap gaseous substitutes [11–14].

In general, natural fibers can be either of plant origin such as Flax [15], bamboo [16], abaca [17] or animal origin such as wool [18] and silk [19]. According to the location of the fibers in the plant, the fibers are classified as: leaf fiber (such as banana fiber [20], pineapple fiber [21]), bast fiber (such as kenaf fiber [22], ramie fiber [23]) and seed fiber (such as cotton fiber [24]). The different types of plant fibers allow some variability in mechanical performance and it also depends on the growing conditions of the plant.

The performance of natural fibers has been analyzed in different studies in order to describe their structure and identify their specific properties. Murali et al. [25] have studied the physical properties of the natural fibers (bamboo, palm tree date, vakka) by determining the length, diameter and density of the fibers. The results show variability in diameter for all the three fibers. The calculated densities of the three fibers are lower than the density of the glass fibers [25]. The chemical composition of vegetable fiber has been studied by infrared spectroscopy in several works. The rigidity of vegetable fiber depends on the cellulosic component of the fiber [26].

After the analysis of the chemical composition of the fiber, the hydrophilicity of the fiber proves to be an interesting property to study by measuring the contact angle and surface energy to identify the appropriate matrix for each fiber to obtain a good adhesion between the reinforcement and the matrix. Singh et al. [27] show that jute fiber shows hydrophilic behavior with a contact angle less than 90° and moisture absorption rate of 14%.

Vegetable yarns made by spinning twisted fibers have been studied in the literature. Corbin et al. [28] have compared the properties of flax yarns and rovings. The results obtained show that the twisting of the yarns improves the tenacity of the yarns at breakage, as well as the irregularity of the yarn properties which is due to the spinning process. Kim and Netravali [29] reveal that the breakage of hemp yarns with a tensile strength of 450 MPa and a linear density of 40.74 Tex propagates around the first broken fibers [29].

The mechanical performance of natural fibers is an important factor in the replacement of synthetic fibers. The tensile properties of natural fibers are tested by two methods either with the unit of the tensile test of the fiber or with the back-calculation of the properties of fibers from the results of the impregnated bundles or yarns using the rule of mixtures [30,31]. Lansiaux et al. [32] have studied the mechanical properties of flax fibers by the Impregnated Fiber Bundle Test (IFBT) method by varying the twist angle of the flax yarns. The obtained results are similar for a twist angle between 0 and 100 tpm with the modified rule of mixtures taking into account the porosity and orientation of the fibers. Among the most efficient natural fibers, sisal fiber is a fiber extracted from the leaves of the agave sisalana plant (Table 1). Thanks to the ease of cultivation of the agave sisalana plant, the production of this fiber represents almost half of the production of textile natural fibers [33,34].

Table 1. Mechanical properties of natural fibers.

Fibers	Tensile Strength (Mpa)	Young Modulus (Gpa)	Failure Strain (%)	References
hemp	40	37.5	2.5	[35]
Coir	131–220	4–6	15–40	[36]
Sisal	468–700	9.4–38	2.0–7.0	[36]
Jute	400–800	10–30	1.16–1.8	[36]
Flax	345–1100	27.6	2.7–3.2	[37]
E-glass	1800–3500	70–73	2.5–3.0	[36]

The sisal fibers are widely cultivated in the tropical and subtropical regions of north and south America and African countries [34–38]. Belaadi et al. [39,40] studied the properties of sisal fiber of Algerian origin. The results prove that the tensile strength and the

Young modulus of the Algerian fibers are superior to the properties of fibers of Indian origin [40]. The growing conditions of each region allow for variability in the performance of the sisal fiber (Table 2). The sisal fiber cultivated in several African countries (precisely in Morocco) is exploited only in traditional medicine. The performance of Moroccan sisal fiber was investigated in a previous study by showing the important mechanical resistance of the Moroccan sisal fiber [41].

Table 2. Mechanical properties of sisal fibers with different origins.

Fiber	Tensile Strength (Mpa)	Young Modulus (GPa)	Fiber Origin	References
Sisal Fiber	391.00 ± 89	10.7 ± 4.0	Brazil	[42]
	462.00 ± 71	7.47 ± 1.37	Algeria	[39]
	294.00 ± 113	9.8 ± 0.9	India	[43]
	340.02 ± 70.4	12.5 ± 7.8	Morocco	[41]
	371 ± 28 MPa	12.43 ± 2.23	Kenya	[44]

This work aims to show the potential of sisal fiber of Moroccan origin for the reinforcement of composite materials at the fiber and yarn scale. This multi-scale approach (fiber/yarn) allows the understanding of the complexity of 2D and 3D fibrous reinforcements. The characterization of sisal yarns is the last step of this study in order to study the smallest entity of the reinforcement. The important factors related to the fiber to assess the adhesion between the matrix and the Moroccan fiber (sisal) were analyzed (hydrophilicity, moisture absorption) according to standards.

2. Materials and Methods

2.1. Materials

Moroccan-Sisal fibers were extracted mechanically from the leaves of the Agave Sisalana plant. After the fiber extraction process, the fibers were washing with distilled water (2 h) and dried in an oven at 40 °C for 24 h [41].

Sisal yarn (Figure 1) was purchased from Moroccan company Sonajute (reference product (300/1 (m/Kg))). It is a simple twisted yarn with a twist level of 80 tpm and a linear density of 3300 Tex.



Figure 1. Moroccan Sisal yarns.

2.2. Characterization of Sisal Fibers

2.2.1. FTIR Analysis

Fourier Transform Infrared analysis was conducted to identify organic and inorganic components of the provided sisal fibers. A Thermo Scientific Smart OMNI-Sampler spectrometer was employed with a wavenumber range from 4000 to 400 cm⁻¹.

2.2.2. Thermogravimetric Analysis (TGA)

The thermal behavior of the sisal fiber was investigated by thermogravimetric analysis operated on TGA-Q500 of TA Instruments (ISO 11358). A sample weighing 5.7 mg of the sisal fibers was heated from 20 °C to 600 °C with a heating rate of 10 °C/min in the nitrogen atmosphere.

2.2.3. Contact Angle Measurement

The wettability of sisal fibers was evaluated by calculating the contact angle θ according to tensiometric method by using a GBX Digidrop (Dublin, Ireland). The fiber was immersed in distilled water with a surface tension of 73.13 (mN/m) at room temperature. The meniscus weight (m) and the wetting perimeter (p) were measured. Then the contact angle was deduced by Equation (1) (Wilhelmy [45]).

$$F = mg = Y_L \times P \times \cos\theta \quad (1)$$

where F is the capillary Force (N), g is the acceleration of gravity ($m.s^{-2}$), Y_L (mN/m) is the surface tension of distilled water, P is the wetting perimeter and θ is the contact angle.

2.2.4. Moisture Absorption Analysis

The moisture absorption analysis consisted of calculating the rate of moisture absorption under the hygrometric conditions indicated in the NF G 08-001-4. A sample weighing 100 g of sisal fibers was dried at 60 °C for 12 h, until a constant mass was reached. Then, the sample was placed in conditioned room ($T = 22$ °C, $RH = 62\%$) and weighted every 15 min until the mass stabilized again. The moisture content in sisal fiber at time t was expressed by the following Equation (2):

$$M_{ma} (\%) = \frac{M_t - M_o}{M_o} \times 100 \quad (2)$$

where M_a (%) is the moisture content of sisal fibers, M_o is the initial weight of samples and M_t is the weight of samples at time t [46].

Fick's law was used to model the moisture diffusion in a composite material by a diffusion coefficient given in Equation (3). This law can be employed to model the moisture diffusion in the inner structure of sisal fiber since it is considered as composite material regarding its composition, cellulosic and non-cellulosic components (lignin, hemicellulose, pectin):

$$D = \frac{\pi}{16} \left(\frac{b}{M_m} \right)^2 \times \left(\frac{M_2 - M_1}{\sqrt{t_2} - \sqrt{t_1}} \right)^2 \quad (3)$$

where D is the Diffusion coefficient, b is the diameter of sisal fiber, M_m is the rate of moisture absorption and M_1 and M_2 are the moisture content at t_1 and t_2 , respectively [47,48].

2.2.5. Fiber Geometry

The morphology of the fiber depends on the length and diameter of the fiber. The diameter was measured using an optical microscope (Olympus BX51, Tokyo, Japan). Twenty-five samples were analyzed through images in the longitudinal direction of the fiber. The average value of the fiber diameter was calculated. The lengths of twenty-five fibers were measured using a special device called a "maillemeter", where one end of the fiber is grasped by a clamp and the second end is attached to a mobile carriage which exerts a force to obtain the real value of the length of the fiber (without any crimp). A longitudinal view of sisal fiber was observed by an electron-scanning microscope (JEOL JSM 6380LA, Jeol Ltd., Tokyo, Japan).

2.2.6. Impregnated Fiber Bundle Test

The mechanical properties of sisal fibers were determined by the Impregnated Fiber Bundle Test (IFBT). The method consists of making composite samples from sisal yarns

and identifying the tensile properties of these samples. Fiber-scale properties are deduced, by inverse computation, thanks to the rule of mixtures [32,33].

Bundles of the sisal fiber were impregnated with an epoxy resin (SR8200/SD7204 sicomin) in a rectangular mold (250 mm × 10 mm). The composite material was pressed using a heating press at 60 °C for 4 h to promote resin curing. Different pressure values were applied in order to investigate the pressure effect on the porosity content in the impregnated samples. Thickness of the composite sample was controlled to 2 mm.

Tensile test was performed on the cured bundle with a speed of 1 mm/min using the Instron 5985 tensile machine with a maximum load of 250 KN. Stiffness of the sisal fibers was determined thanks to the modified rule of mixtures [49,50], as given in Equation (4). In comparison with the classic rule of mixtures, the modified formulae take into account the porosity content in composite samples in addition to the two associated factors, respectively, fiber orientation and fiber length.

$$E_c = (\eta_0 \eta_1 V_f E_f + V_m E_m) \times (1 - V_p)^n \quad (4)$$

where:

- E_f , E_c and E_m are the stiffness of fibers, composites and the matrix, respectively.
- V_f , V_m and V_p are the volume fraction of fibers, the matrix and porosity, respectively.
- n is the porosity efficiency exponent. If $n = 0$, Equation (4) does not consider the level of porosity and will be denoted here as rule of mixtures R1. $n = 2$ corresponds to the general value of the composites based on natural fibers (denoted here, rule of mixtures R2).
- η_0 is the fiber orientation efficiency factor.
- η_1 is the fiber length efficiency factor ($\eta_1 = 1$ [30,48,49]).

The fiber orientation efficiency factor can be expressed either as a function of linear density of yarns and density of sisal fiber, given by Equation (5) (Rule of mixtures R3) or as a function of the twist angle of the sisal yarns [4–6], given by Equation (6) (Rule of mixture R4).

$$\eta_0 = \cos(2 * \tan^{-1}(10^{-3} \cdot T \sqrt{4\pi \cdot \frac{L}{\rho \cdot \varphi}})) \varphi = 0.7 \times (1 - 0.78e^{-0.195T}) \quad (5)$$

with

$$\eta_0 = \cos^2 2\alpha \quad (6)$$

where:

- ρ is the density of Moroccan sisal fibers (1.45 kg/m³);
- L is the linear density of sisal yarns (3300 Tex);
- T is the twist level in tpm (turns per meters);
- φ is the fiber packing factor [49,50];
- and α is the twist angle [49,50].

From these models, stiffness of the sisal fibers was computed by inverse computation from the properties of the elaborated composites in two ranges of deformation: between 0 and 0.1% for the first modulus, denoted E1f and between 0.3 and 0.5% for the second modulus, denoted E2f.

2.3. Characterization of Sisal Yarns

2.3.1. Diameter and Linear Density Measurement

The yarns were conserved in lab conditions (21 °C, 65% for 24 h). The diameter of sisal yarns was measured using the mini optical microscope. Twenty-five samples of yarns with a length of 40 mm were visualized and the average value of their diameters was calculated. The linear density of sisal yarns was measured according to ISO 1889. Furthermore, the

angle of the fiber located on the outer surface of the yarn was measured with the aid of captured pictures taken on the optical microscope and using ImageJ software.

2.3.2. Tensile Analysis

The tensile behavior of sisal yarns was investigated according to NF ISO 2062 by a tensile tester (MTS SYSTEM) with a maximal load 10KN. Twenty specimens of yarns were tested with a gauge length of 100 mm at room temperature.

3. Results and Discussion

3.1. FTIR spectroscopy of Sisal Fibers

Different spectral bands describing the chemical composition of the sisal fiber are shown in Figure 2. The first band between 3200 and 3500 cm^{-1} is attributed to an O-H group showing the presence of hemicellulose and cellulose. The peak identified between 2900 and 3100 cm^{-1} corresponds to a C-H group bound to cellulose and hemicellulose. These two bands represent both the macromolecular interactions of cellulose and hemicellulose as well as the presence of water in the fibers, both of which promote the binding of water molecules to these characteristic hydroxyl groups. The C-H Stretching vibration region at the band level around 1735 cm^{-1} is due to the hemicellulosic component. Shear vibration of the OH-bond illustrates the presence of free water in the fiber structure. Pectin constituting the fiber appears at the vibration of the carboxyl bond between 1430 and 1420 cm^{-1} . The carboxyl functions of pectins which make up the middle lamella, are also impacted by absorption of water. Stretching of the C-O bonds at the 1225 cm^{-1} peak identifies the presence of lignin. The cellulose is shown by stretching the C-O-C bond at wavelength 1023 cm^{-1} which is the characteristic of the polysaccharide nature of the fiber. This signature is also impacted by the increase in humidity [51–53]. The infrared spectrum of the fiber shows the ability of the fiber to absorb moisture due to its chemical composition [54].

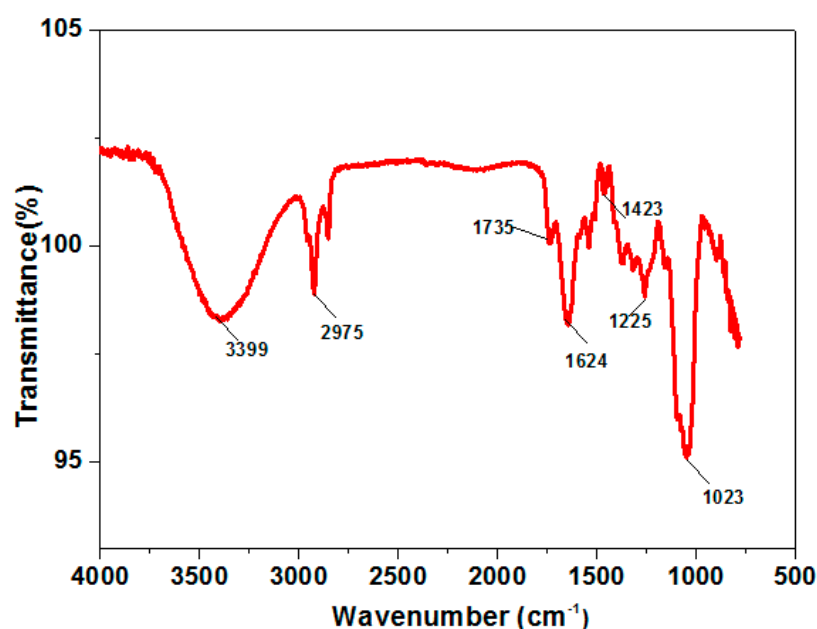


Figure 2. FTIR spectrum of Sisal Fibers.

3.2. Thermal Behavior of Sisal Fibers

The thermal behavior of the sisal fiber is illustrated in Figure 3. The first phase is dehydration of the fiber. The dehydration phase takes place between 50 °C and 150 °C while the dehydration is linked to the chemical structure of the fiber components (cellulose, hemicellulose). The components of the fiber (cellulose, hemicellulose) occur between 150 °C and 200 °C. The weight loss at the dehydration phase is 9.67% of the sample weight. The second

phase involves the degradation of hemicellulose in view of its branch-rich amorphous structure which facilitates the degradation of its constituents. The decomposition temperature is between 201 °C and 320 °C [55,56]. The weight loss at the decomposition of hemicellulose is 20.9%. The third phase is related to the degradation of the cellulose. It is due to the cleavage of the glycosidic linkage of the cellulosic component in the fiber [57,58]. The last decomposition phase occurs between 390 °C and 475 °C is attributed to free radicals at oxidative atmosphere. The sisal fiber residue at 600 °C is 10.56%. The temperature range of the thermal degradation of the fiber components (cellulose, hemicellulose and lignin) corresponds to the same range of the decomposition of thermoplastic and thermosetting resins [59]. The sisal fiber is resistant to a temperature of 220 °C with a residual mass of 3%. The sensitivity to temperature of the sisal fiber is an important factor in the processing of composite materials based on this fiber.

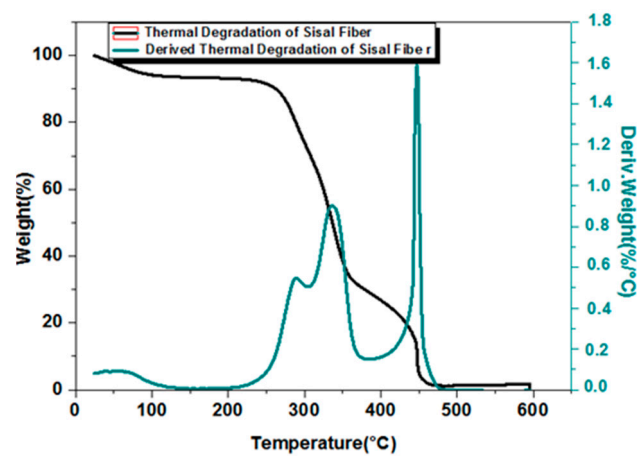


Figure 3. Thermogravimetric analysis curve of Sisal Fibers.

3.3. Contact Angle of Sisal Fibers

Hydrophobicity of the sisal fiber is determined by measuring the contact angle with distilled water. Hydrophobic material is characterized by a T contact angle exceeding 90°, whereas this angle is less than 90° for a hydrophilic material. The contact angle on the surface of the tested sisal fiber is 53.06°; Table 3 lists the obtained result in comparison with Flax and Jute fibers. In general, the natural fibers in the presence of lignocellulosic constituents promote water absorption by hydroxyl groups. Otherwise, this observed hydrophilicity property of the sisal fiber limits its use as reinforcement with a non-polar hydrophobic matrix due to poor interfacial adhesion [60]. The hydrophilicity of the sisal fiber shows the capacity of the fiber to bind water molecules. This factor is very important for the choice of the right matrix for the structure of the fiber.

Table 3. Contact Angle of Sisal Fiber.

Fibers	Surface Tension of Distilled Water γ_L (mN/m)	Contact Angle (°)	References
Sisal Fiber	73.13	53.06	Current Study
Flax Fiber	73.13	41.5	[61]
Jute Fiber	73.13	63.9	[62]

3.4. Moisture Absorption

Evolution of moisture absorption in the sisal fiber is illustrated in Figure 4. The hydrophilicity and the hygroscopic property of sisal fiber favor moisture absorption with a rate of 13.6% by mass. Sisal fiber shows more attractive moisture behavior than ramie fiber with a recovery rate of 6% [63]. The moisture absorption by the fiber passes through

two phases: the first phase corresponds to the absorption of moisture due to capillary action because of the porous structure of the fiber; this phase is shown by the linear part of the absorption curve (Figure 4). The second phase is characterized by the concave part of the curve explained by the change in the internal structure of the fiber due to the fiber swelling. The absorption of moisture in the sisal fiber contributes to the insertion of water molecules between the molecules of the fiber constituents, which affects the interactions between the cellulose fibrils and the pectin matrix and thus the modulus [64].

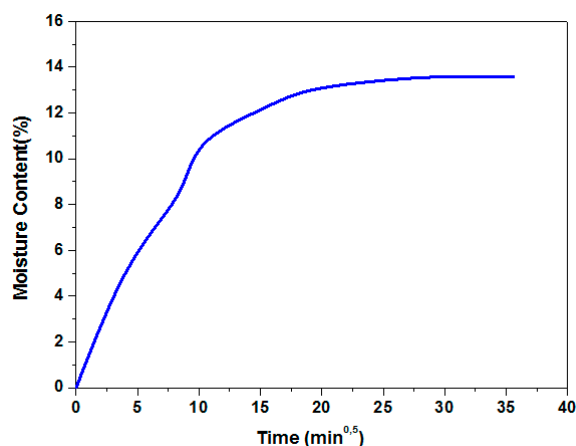


Figure 4. Moisture absorption of Sisal fibers.

The diffusion coefficient defined by Fick law is determined for the moisture absorption in sisal fiber. The fiber is modelled as a cylindrical shaped material according to the Equation (3). The diffusion coefficient of the sisal fiber is $1.77 \times 10^{-4} \text{ mm}^2/\text{s}$. The diffusion coefficients of the jute and flax fibers tested by Céline et al. are listed in Table 4 [46]. The difference between the moisture absorption capacity of sisal fiber and jute fiber is due to the higher hydrophobicity of sisal fiber (contact angle 53.06°) compared to the hydrophobicity of jute fiber (contact angle 63.9° [62]). However, the Moisture absorption capacity of natural fibers is a parameter affecting the long-term mechanical performance of composites.

Table 4. Diffusion parameters of Sisal fibers according to the Fick law.

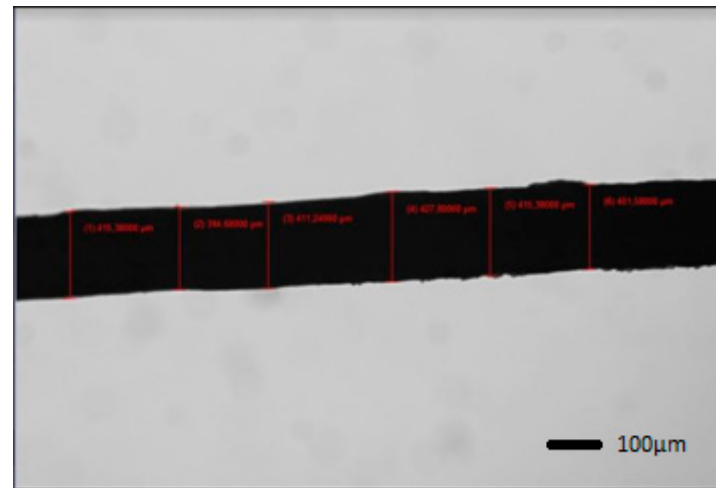
Fiber	Diffusion Coefficient (mm^2/s)	Permeability Coefficient (mm^2/s)	Moisture Content at t_∞ (%)	References
Sisal Fiber	1.77×10^{-4}	2.00×10^{-4}	13.6	Current Study
Flax Fiber	2.00×10^{-4}	-	12.0	[46]
Jut Fiber	4.02×10^{-4}	-	12.3	[46]

3.5. Structural Fiber Geometry

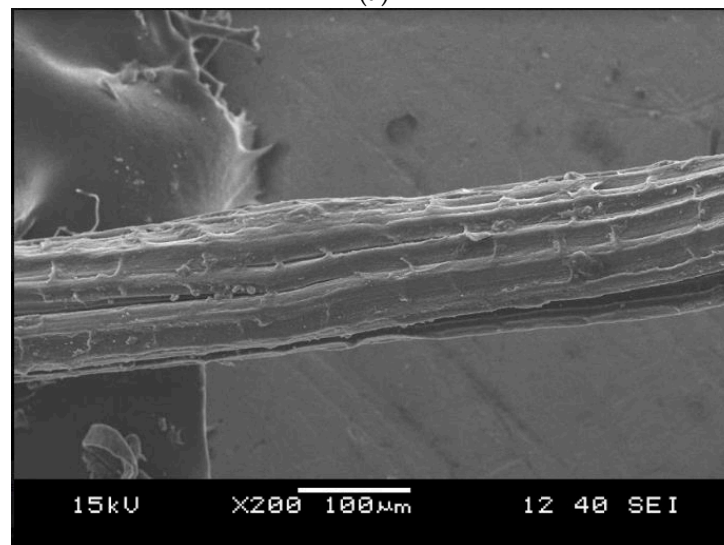
The length and diameter of sisal fiber were measured to determine the fiber consistency and fitness. The length of sisal fibers (Table 5) shows a variability that depends on the morphology and the extraction method of the fiber. The average value of sisal fiber was $74.5 \pm 30.23 \text{ mm}$. The length of the sisal fiber is small compared to the length of the ramie fiber, which is between 50 and 110 mm [64]. The diameter of the sisal fiber is around $121.6\text{--}411.0 \text{ }\mu\text{m}$ (Figure 5a). The sisal fiber shows an irregular diameter like other vegetable fibers, unlike the uniform shape of synthetic fibers such as glass fiber. The structure of the fiber (Figure 5b) visualized by the scanning electron microscope shows the rough surface consisting of micro fibrils. The nature of the surface of the sisal fiber is due to the presence of impurities (oil, pectin, wax). The surface of the raw fiber can be an obstacle for the good adhesion between the fiber and the matrix. This problem can be solved by the chemical treatments of the fiber (alkaline) [65].

Table 5. Dimensions of Sisal fibers.

Length Interval (mm)	Average Length (mm)	Diameter Interval (μm)	Average Diameter (μm)
50–110	74.5 ± 30.23	121.6–411.0	239.0 ± 80.18



(a)



(b)

Figure 5. Optical and SEM images of Sisal fiber: (a) optical image of Sisal fiber; (b) SEM image of Sisal fiber.

3.6. Tensile Properties of Sisal Fibers

The tensile properties of sisal fibers were evaluated using the IFBT Test. The fiber volume fraction of the prepared impregnated samples is about 43.62% as an average with a consideration of the fiber density to 1.45 g/cm^3 . The porosity content in these samples was also assessed and low porosity was obtained with about 4.12% as an average. Porosities can be observed on a micrograph made on the cross section of the sample, Figure 6, and located inter the fiber-bundles (yarns). In addition, porosities of smaller size are observed inside the bundles and at the matric–bundle interface. However, the micrograph shows penetration of the resin inside the fiber bundles.

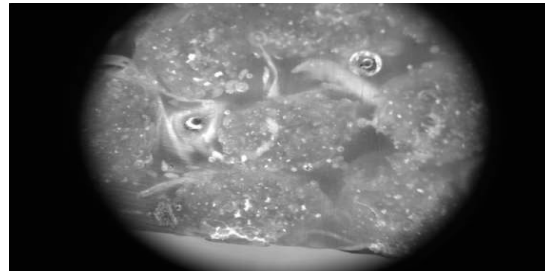


Figure 6. Cross sectional images of specimens of the IFBT method.

The elastic modulus of the sisal fibers is back-calculated from the three modified rules of mixtures (Equations (4)–(6)) in addition to the standard rule of mixtures. The elastic modulus of used epoxy resin is $E_{av} = 3$ GPa. Figure 7 shows that a significant variation in the modulus values of E_{1f} and E_{2f} by the different rules of mixtures. The elastic modulus back-calculated by the modified rule of mixtures R4 taking into account the porosity content and the fiber orientation gives the upper value of the modulus E_{1f} and E_{2f} . The back-calculated values of the modulus E_{1f} and E_{2f} from different equations are between 9 and 18 GPa. These results are in accordance with other works studying the elementary single fiber testing of sisal fibers [39,66–68].

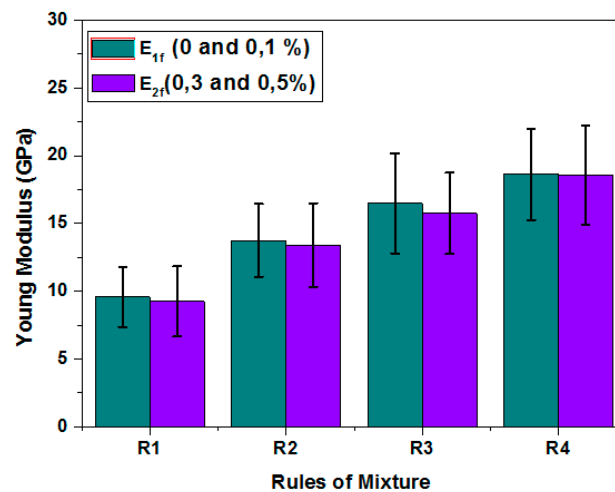


Figure 7. Young modulus of Moroccan Sisal fibers by the Impregnated Fiber Bundle Test (IFBT) method.

The tensile modulus of sisal fiber from different origins (Table 6) shows that the range of values of the elastic modulus of the sisal fiber with Indian origin is similar to the range of the elastic modulus from Moroccan origin analyzed in the current study. The elastic modulus of the flax fiber has been studied by Lansiaux et al. [30] using IFBT method and back-calculated from the rule of mixtures R3 using twisted flax yarns with a twist level between 0 and 100 tpm, the value obtained is around 30 GPa.

Table 6. Elastic modulus of Sisal fibers from different origins.

Fiber	Origin	Elastic Modulus (Gpa)	Method of Testing	References
Sisal Fiber	Brazil	10.7 ± 4.0	Tensile Test of elementary Fiber	[42]
	Algeria	7.47 ± 1.37	Tensile Test of elementary Fiber	[39]
	India	9.8 ± 0.9	Tensile Test of elementary Fiber	[43]
	Morocco	12.5 ± 7.8	Tensile Test of elementary Fiber	[41]
	Morocco	17.02 ± 3.74	IFBT Method	Current Study

3.7. Diameter and Linear Density of Sisal Yarns

The sisal yarn is made of a bundle of z-twisted fibers with a twist level about 80 tpm, Figure 8. Mostly, the yarns are z-twisted because the spinning machines are made for right-handed manipulators [69]. The average value of the sisal yarns' diameter is 2.01 ± 0.9 mm (Table 7). The average value of the linear density of the sisal yarns is around 3.3 ± 0.7 kTex. The variability of the linear density along the yarn is due to the irregular value of twisted sisal fibers diameter. This variability is due to the variability of the climatic conditions and the cultivation conditions of the plant. The sisal yarns with Algerian origin were studied by Belaadi et al. [70] and the obtained results show that the average diameter value is 2.04 ± 0.26 mm.

**Figure 8.** Image of Sisal yarns.**Table 7.** Properties of Sisal yarns.

Yarn	Average Diameter (mm)	Average Linear Density (Ktex)	Twist Level (Tpm)
Sisal Yarn	2.01 ± 0.9	3.3 ± 0.7	80

The twist angle of the sisal yarns was calculated theoretically based on the fiber orientation factor which can be expressed as a function of the twist angle α on the outer surface of the yarn (Equation (6)) [49,50].

α is evaluated by two methods with the assumption of circular cross-section shape of the twisted yarn:

Method 1: the section of the yarn is not considered to be full of fibers (Equation (5)) (see Section 2.2.6.). The fibers are packed in the yarn section can be expected to behave according to the semi-empirical model proposed by Pan [49,50], and given by Equation (5).

Thus, the fiber twist angle on the outer surface of the yarn is computed by Equation (7).

$$\alpha = \tan^{-1} \left(T 10^{-3} \sqrt{\frac{4\pi kTex}{\rho \phi}} \right) \quad (7)$$

Method 2: the section of the yarn is considered full of fibers so the fiber packing factor in the yarn section is equal to one and the fiber twist angle is computed by Equation (8):

$$\alpha = \tan^{-1} \left(T 10^{-3} \sqrt{\frac{4\pi kTex}{\rho}} \right) \quad (8)$$

where:

- ρ is the density of Moroccan sisal fibers (1.45 kg/m³).
- T is the twist level in tpm (turns per meters).
- $kTex$ is the linear density of yarns (Ktex).

The twist angle of the sisal yarns was calculated based on the two configurations of the yarn cross-section. The twist angle of the yarns obtained with a packing factor is 26.92°, while the twist angle without a packing factor is 23.16°. From the elaborated samples of the IFBT method (Section 2.2.6.), the packing factor was verified by an Equation by measuring the yarn cross-sectional area in Figure 7.

The Yarn Packing Factor:

$$\phi = \frac{kTex}{\rho A_{fil}} \quad (9)$$

where:

- ρ is the density of Moroccan sisal fibers (1.45 kg/m³).
- $kTex$ is the linear density of yarns (Ktex).
- A_{fil} is the yarn cross-sectional area (m²).

The yarn packing factor is 70.2% with a standard deviation of 5.63%. With this packing factor verification, the yarn twist angle is 23.65 ± 3.65°. In order to evaluate the accuracy of the different methods, the twist angle was measured from the yarn pictures using the ImageJ software (Figure 9), the value obtained is 23.14° with a standard deviation of 2.75°. The obtained results (Table 8) show that the twist angle calculated by both methods is included in the range of variation of the measured twist angle.



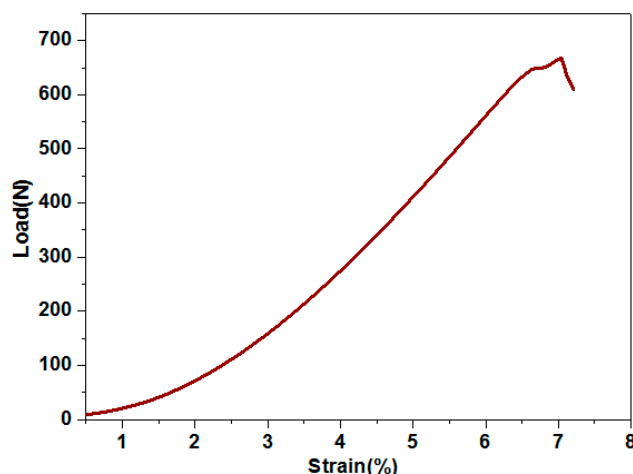
Figure 9. Sisal yarn with measurement for twist angle by ImageJ software (experimental method).

Table 8. Twist angle of Sisal yarn.

Sisal Yarns	Method 1 (Theoretical Method with Packing Factor)	Method 2 (Theoretical Method without Packing Factor)	Verification Method Based on the IFBT Samples	Experimental Method
Twist Angle	26.92°	23.16°	24.16 ± 3.65°	23.14 ± 2.75°

3.8. Tensile Behavior of Sisal Yarns

The tensile properties of sisal yarns were studied under quasi-static loading. Figure 10 shows load versus strain of sisal yarns. The curves can be divided into two zones, the first zone is non-linear between 1 and 4% of the deformation value, which can be explained by the realignment of the twisted fibers during the tensile test, which creates a space between the fibers in the yarn structure [71]. The second zone is quasi-linear between 4 and 7% of the deformation before yarn breakage. The observed behavior of the sisal yarns of Moroccan origin studied in this work is similar to the behavior of sisal yarns of Algerian origin [70] and flax yarns [71].

**Figure 10.** Average load—strain curve of Sisal yarns.

The average value of the maximum load is 672.36 ± 236 N. The dispersion of the results of this test is due to the variability of the properties of the sisal fibers. The average value of the tenacity of sisal yarns is 20.24 cN/Tex (± 3.25) (Table 9). The tenacity of sisal yarns of Indian origin is of the order of 18.38 cN/Tex with a maximum strength of 514.7 N [72]. The difference in the mechanical properties of the sisal yarns according to the origin depends on the climatic and growing conditions of the agave sisalana plant in different regions.

Table 9. Tenacity of natural yarns.

Yarns	Tenacity (cN/Tex)	References
Sisal	20.24 ± 3.25	Current Study
Sisal	18.38 ± 2.97	[28]
Coir	14.00 ± 4.68	[29]

4. Conclusions

This work aims to analyze the physical and mechanical properties of sisal fibers and yarns of Moroccan origin. The chemical composition of the fiber contains cellulosic elements that promote a mechanical performance of the reinforcement of the composite

material. The thermogravimetric analysis of sisal fiber shows a low thermal stability. The presence of the hydroxyl groups (OH) in the structure of the fiber favors the hydrophilic behavior of the fiber, with a contact angle of 53.06°. The moisture absorption rate of the fiber is 13.2%. The mechanical properties of the fiber analyzed by the IFBT method shows that the porosity of the impregnated yarns and the twist angle of the yarns influence the elastic modulus of sisal fiber. The physical and mechanical properties of sisal yarns show a variability in the values of diameter and a linear density that depends on the properties of the twisted fibers used in the spinning process. This investigation on the properties of sisal fiber of Moroccan origin proves that this fiber can be an alternative fiber to synthetic fibers because of its recyclability, low density, eco-friendly and its abundance in several regions, which are highly demanded points in the strategy of sustainable development. The limitations of the fiber such as moisture absorption and low thermal stability can be optimized for the development of reinforcements of composite materials.

Author Contributions: Investigation: Z.S.; writing—original draft preparation: Z.S.; validation; supervision: F.B., D.S., A.R.L., R.E.m.; writing—review and editing: F.B., D.S. and A.R.L.; funding acquisition: O.C. and F.B. All authors have read and agreed to the published version of the manuscript.

Funding: This research was financially supported by Ministry of Europe and Foreign Affairs, Ministry of Higher Education, Research and Innovation and the French Institute of Rabat (PHC TOUBKAL 2019/83 (French–Morocco bilateral program) Grant Number: 41511ZF.

Institutional Review Board Statement: Not applicable.

Informed Consent Statement: Not applicable.

Data Availability Statement: Not applicable.

Conflicts of Interest: The authors declare no conflict of interest.

References

1. La Mantia, F.P.; Morreale, M. Green composites: A brief review. *Compos. Part A Appl. Sci. Manuf.* **2011**, *42*, 579–588. [[CrossRef](#)]
2. Zini, E.; Scandola, M. Green composites: An overview. *Polym. Compos.* **2011**, *32*, 1905–1915. [[CrossRef](#)]
3. Dicker, M.P.; Duckworth, P.F.; Baker, A.B.; François, G.; Hazzard, M.K.; Weaver, P.M. Green composites: A review of material attributes and complementary applications. *Compos. Part A Appl. Sci. Manuf.* **2014**, *56*, 280–289. [[CrossRef](#)]
4. Fowler, P.A.; Hughes, J.M.; Elias, R.M. Biocomposites: Technology, environmental credentials and market forces. *J. Sci. Food Agric.* **2006**, *86*, 1781–1789. [[CrossRef](#)]
5. Gurunathan, T.; Mohanty, S.; Nayak, S.K. A review of the recent developments in biocomposites based on natural fibers and their application perspectives. *Compos. Part A Appl. Sci. Manuf.* **2015**, *77*, 1–25. [[CrossRef](#)]
6. Satyanarayana, K.G.; Arizaga, G.G.C.; Wypych, F. Biodegradable composites based on lignocellulosic fibers—An overview. *Prog. Polym. Sci.* **2009**, *34*, 982–1021. [[CrossRef](#)]
7. Ravi, M.; Dubey, R.R.; Shome, A.; Guha, S.; Kumar, C.A. Effect of surface treatment on Natural fibers composite. *IOP Publ.* **2018**, *376*. [[CrossRef](#)]
8. Joshi, S.V.; Drzal, L.T.; Mohanty, A.K.; Arora, S. Are natural fiber composites environmentally superior to glass fiber reinforced composites? *Compos. Part A Appl. Sci. Manuf.* **2004**, *35*, 371–376. [[CrossRef](#)]
9. Wu, Y.; Xia, C.; Cai, L.; Garcia, A.C.; Shi, S.Q. Development of natural fiber-reinforced composite with comparable mechanical properties and reduced energy consumption and environmental impacts for replacing automotive glass-fiber sheet molding compound. *J. Clean. Prod.* **2018**, *184*, 92–100. [[CrossRef](#)]
10. Biswas, S.; Satapathy, A. A comparative study on erosion characteristics of red mud filled bamboo-epoxy and glass-epoxy composites. *Mater. Des.* **2010**, *31*, 1752–1767. [[CrossRef](#)]
11. Mohammed, L.; Ansari, M.N.; Pua, G.; Jawaid, M.; Islam, M.S. A review on natural fiber reinforced polymer composite and its applications. *Int. J. Polym. Sci.* **2015**, *2015*. [[CrossRef](#)]
12. Gallo, E.; Schartel, B.; Acierno, D.; Cimino, F.; Russo, P. Tailoring the flame retardant and mechanical performances of natural fiber-reinforced biopolymer by multi-component laminate. *Compos. Part B Eng.* **2013**, *44*, 112–119. [[CrossRef](#)]
13. Sanjay, M.R.; Siengchin, S.; Parameswaranpillai, J.; Jawaid, M.; Pruncu, C.I.; Khan, A. A comprehensive review of techniques for natural fibers as reinforcement in composites: Preparation, processing and characterization. *Carbohydr. Polym.* **2019**, *207*, 108–121.
14. Kim, H.S.; Lee, B.H.; Kim, H.J.; Yang, H.S. Mechanical-thermal properties and VOC emissions of natural-flour-filled biodegradable polymer hybrid bio-composites. *J. Polym. Environ.* **2011**, *19*, 628–636. [[CrossRef](#)]

15. Lansiaux, H.; Soulat, D.; Boussu, F.; Labanieh, A.R. Manufacture and Characterization of 3D Warp Interlock Fabric Made of Flax Roving. In Proceedings of the 13th International Conference on Textile Composites (TEXCOMP-13), Milan, Italy, 17–19 September 2018.
16. Mounika, M.; Ramaniah, K.; Prasad, A.R.; Rao, K.M.; Reddy, K.H.C. Thermal conductivity characterization of bamboo fiber reinforced polyester composite. *J. Mater. Environ. Sci.* **2012**, *3*, 1109–1116.
17. Cai, M.; Takagi, H.; Nakagaito, A.N.; Li, Y.; Waterhouse, G.I. Effect of alkali treatment on interfacial bonding in abaca fiber-reinforced composites. *Compos. Part A Appl. Sci. Manuf.* **2016**, *90*, 589–597. [[CrossRef](#)]
18. Zihlif, A.M.; Ragosta, G. A study on the physical properties of rock wool fiber—Polystyrene composite. *J. Thermoplast. Compos. Mater.* **2003**, *16*, 273–283. [[CrossRef](#)]
19. Yuan, Q.; Yao, J.; Chen, X.; Huang, L.; Shao, Z. The preparation of high performance silk fiber/fibroin composite. *Polymer* **2010**, *51*, 4843–4849. [[CrossRef](#)]
20. Pothan, L.A.; Oommen, Z.; Thomas, S. Dynamic mechanical analysis of banana fiber reinforced polyester composites. *Compos. Sci. Technol.* **2003**, *63*, 283–293. [[CrossRef](#)]
21. Devi, L.U.; Bhagawan, S.S.; Thomas, S. Mechanical properties of pineapple leaf fiber-reinforced polyester composites. *J. Appl. Polym. Sci.* **1997**, *64*, 1739–1748. [[CrossRef](#)]
22. Akil, H.; Omar, M.F.; Mazuki, A.A.M.; Safiee, S.Z.A.M.; Ishak, Z.M.; Bakar, A.A. Kenaf fiber reinforced composites: A review. *Mater. Des.* **2011**, *32*, 4107–4121. [[CrossRef](#)]
23. Yu, T.; Ren, J.; Li, S.; Yuan, H.; Li, Y. Effect of fiber surface-treatments on the properties of poly (lactic acid)/ramie composites. *Compos. Part A Appl. Sci. Manuf.* **2010**, *41*, 499–505. [[CrossRef](#)]
24. Kim, S.J.; Moon, J.B.; Kim, G.H.; Ha, C.S. Mechanical properties of polypropylene/natural fiber composites: Comparison of wood fiber and cotton fiber. *Polym. Test.* **2008**, *27*, 801–806. [[CrossRef](#)]
25. Rao, K.M.M.; Rao, K.M. Extraction and tensile properties of natural fibers: Vakka, date and bamboo. *Compos. Struct.* **2007**, *77*, 288–295. [[CrossRef](#)]
26. Komuraiah, A.; Kumar, N.S.; Prasad, B.D. Chemical composition of natural fibers and its influence on their mechanical properties. *Mech. Compos. Mater.* **2014**, *50*, 359–376. [[CrossRef](#)]
27. Singh, B.; Gupta, M.; Tarannum, H.; Randhawa, A. Natural Fiber-Based Composite Building Materials. In *Cellulose Fibers: Bio-and Nano-Polymer Composites*; Kalia, S., Kaith, B.S., Kaur, I., Eds.; Springer: Berlin/Heidelberg, Germany, 2011; pp. 154–196.
28. Corbin, A.C.; Boussu, F.; Ferreira, M.; Soulat, D. Influence of 3D warp interlock fabrics parameters made with flax rovings on their final mechanical Behavior. *J. Ind. Text.* **2020**, *49*, 1123–1144. [[CrossRef](#)]
29. Kim, J.T.; Netravali, A.N. Development of aligned-hemp yarn-reinforced green composites with soy protein resin: Effect of pH on mechanical and interfacial properties. *Compos. Sci. Technol.* **2011**, *71*, 541–547. [[CrossRef](#)]
30. Prapavesis, A.; Tojaga, V.; Östlund, S.; van Vuure, A.W. Back calculated compressive properties of flax fibers utilizing the Impregnated Fiber Bundle Test (IFBT). *Compos. Part A Appl. Sci. Manuf.* **2020**, *135*, 105930. [[CrossRef](#)]
31. Bensadoun, F.; Verpoest, I.; Baets, J.; Müssig, J.; Graupner, N.; Davies, P.; Gomina, M.; Kervoelen, A.; Baley, C. Impregnated fiber bundle test for natural fibers used in composites. *J. Reinf. Plast. Compos.* **2017**, *36*, 942–957. [[CrossRef](#)]
32. Lansiaux, H.; Soulat, D.; Boussu, F.; Labanieh, A.R. Development and Multiscale Characterization of 3D Warp Interlock Flax Fabrics with Different Woven Architectures for Composite Applications. *Fibers* **2020**, *8*, 15. [[CrossRef](#)]
33. Mukherjee, P.S.; Satyanarayana, K.G. Structure and properties of some vegetable fibers. *J. Mater. Sci.* **1984**, *19*, 3925–3934. [[CrossRef](#)]
34. Mishra, S.; Mohanty, A.K.; Drzal, L.T.; Misra, M.; Hinrichsen, G. A review on pineapple leaf fibers, sisal fibers and their biocomposites. *Macromol. Mater. Eng.* **2004**, *289*, 955–974. [[CrossRef](#)]
35. Mwaikambo, L.A.; Ansell, M.P. Mechanical properties of alkali treated plant fibers and their potential as reinforcement materials. I. Hemp fibers. *J. Mater. Sci.* **2006**, *41*, 2483–2496. [[CrossRef](#)]
36. Jayabal, S.; Gurusideswar, S. Comparison of Mathematical Model and ANN Model for the prediction of Thrust and Torque forces in drilling of NFRC. In Proceedings of the 2nd National Conference on “Advances in Mechanical Sciences”, Coimbatore, India, 27–28 March 2008.
37. Malkapuram, R.; Kumar, V.; Negi, Y.S. Recent development in natural fiber reinforced polypropylene composites. *J. Reinf. Plast. Compos.* **2009**, *28*, 1169–1189. [[CrossRef](#)]
38. Chand, N.; Tiwary, R.K.; Rohatgi, P.K. Bibliography resource structure properties of natural cellulosic fibers—An annotated bibliography. *J. Mater. Sci.* **1988**, *23*, 381–387. [[CrossRef](#)]
39. Belaadi, A.; Bezazi, A.; Bouchak, M.; Scarpa, F. Tensile static and fatigue Behavior of sisal fibers. *Mater. Des.* **2013**, *46*, 76–83. [[CrossRef](#)]
40. Belaadi, A.; Bezazi, A.; Bouchak, M.; Scarpa, F.; Zhu, C. Thermochemical and statistical mechanical properties of natural sisal fibers. *Compos. Part B Eng.* **2014**, *67*, 481–489. [[CrossRef](#)]
41. Samouh, Z.; Molnar, K.; Boussu, F.; Cherkaoui, O.; El Moznine, R. Mechanical and thermal characterization of sisal fiber reinforced polylactic acid composites. *Polym. Adv. Technol.* **2019**, *30*, 529–537. [[CrossRef](#)]
42. de Andrade Silva, F.; Chawla, N.; de Toledo Filho, R.D. Tensile Behavior of high performance natural (sisal) fibers. *Compos. Sci. Technol.* **2008**, *68*, 3438–3443. [[CrossRef](#)]

43. Pappu, A.; Pickering, K.L.; Thakur, V.K. Manufacturing and characterization of sustainable hybrid composites using sisal and hemp fibers as reinforcement of poly (lactic acid) via injection moulding. *Ind. Crop. Prod.* **2019**, *137*, 260–269. [[CrossRef](#)]
44. Okeola, A.A.; Abuodha, S.O.; Mwero, J. Experimental investigation of the physical and mechanical properties of Sisal fiber-reinforced concrete. *Fibers* **2018**, *6*, 53. [[CrossRef](#)]
45. Moghaddam, M.S.; Claesson, P.M.; Wälinder, M.E.; Swerin, A. Wettability and liquid sorption of wood investigated by Wilhelmy plate method. *Wood Sci. Technol.* **2014**, *48*, 161–176. [[CrossRef](#)]
46. Céline, A.; Fréour, S.; Jacquemin, F.; Casari, P. Characterization and modeling of the moisture diffusion Behavior of natural fibers. *J. Appl. Polym. Sci.* **2013**, *130*, 297–306. [[CrossRef](#)]
47. Ho Thi, T.N. Étude de L'influence de la Température et de L'humidité sur les Propriétés Mécaniques en Traction des Fibres de Chanvre et de Coco. Ph.D. Thesis, École de Technologie Supérieure, Montreal, QC, Canada, 28 April 2008.
48. Gudayu, A.D.; Steuernagel, L.; Meiners, D.; Gideon, R. Effect of surface treatment on moisture absorption, thermal, and mechanical properties of sisal fiber. *J. Ind. Text.* **2020**. [[CrossRef](#)]
49. Shah, D.U.; Schubel, P.J.; Clifford, M.J. Modelling the effect of yarn twist on the tensile strength of unidirectional plant fiber yarn composites. *J. Compos. Mater.* **2013**, *47*, 425–436. [[CrossRef](#)]
50. Madsen, B.; Thygesen, A.; Lilholt, H. Plant fiber composites-porosity and stiffness. *Compos. Sci. Technol.* **2009**, *69*, 1057–1069. [[CrossRef](#)]
51. Fan, M.; Dai, D.; Huang, B. Fourier Spectroscopy for Natural Fibers Transform Infrared. In *Fourier Transform Materials Analysis*; Salih, S., Ed.; Intech: Rijeka, Croatia, 2012; pp. 45–68.
52. Hinterstoisser, B.; Salmén, L. Application of dynamic 2D FTIR to cellulose. *Vib. Spectrosc.* **2000**, *22*, 111–118. [[CrossRef](#)]
53. Srivastava, H.C.; Adams, G.A. Uronic Acid Components of Jute Fiber Hemicellulose. *J. Am. Chem. Soc.* **1959**, *81*, 2409–2412. [[CrossRef](#)]
54. Céline, A.; Gonçalves, O.; Jacquemin, F.; Fréour, S. Utilisation de la spectrométrie infrarouge pour une quantification rapide du taux d'humidité dans des fibres végétales. *Rev. Compos. Matériaux Av.* **2014**, *24*, 81–95. [[CrossRef](#)]
55. Orfão, J.J.; Antunes, F.J.; Figueiredo, J.L. Pyrolysis kinetics of lignocellulosic materials—Three independent reactions model. *Fuel* **1999**, *78*, 349–358. [[CrossRef](#)]
56. Poletto, M.; Júnior, H.L.O.; Zattera, A.J. Thermal Decomposition of Natural Fibers: Kinetics and Degradation Mechanisms. In *Reactions and Mechanisms in Thermal Analysis of Advanced Materials*; Tiwari, A., Raj, B., Eds.; Wiley & Sons: Hoboken, NJ, USA, 2015; pp. 515–545.
57. Antal, M.J.; Varhegyi, G.; Jakab, E. Cellulose pyrolysis kinetics: Revisited. *Ind. Eng. Chem. Res.* **1998**, *37*, 1267–1275. [[CrossRef](#)]
58. Grønli, M.G.; Várhegyi, G.; Di Blasi, C. Thermogravimetric analysis and devolatilization kinetics of wood. *Ind. Eng. Chem. Res.* **2002**, *41*, 4201–4208. [[CrossRef](#)]
59. Lau, K.T.; Hung, P.Y.; Zhu, M.H.; Hui, D. Properties of natural fiber composites for structural engineering applications. *Compos. Part B Eng.* **2018**, *136*, 222–233. [[CrossRef](#)]
60. John, M.J.; Anandjiwala, R.D. Recent developments in chemical modification and characterization of natural fiber-reinforced composites. *Polym. Compos.* **2008**, *29*, 187–207. [[CrossRef](#)]
61. Pucci, M.F.; Liotier, P.J.; Drapier, S. Caractérisation de la Mouillabilité de Fibers—Application aux Fibers Naturelles. Characterization of Fiber Wettability—Application to Natural Fibers. In *Proceedings of the Comptes Rendus des JNC 20—École des Ponts ParisTech*, Paris, France, 28–30 June 2017.
62. Roy, A.; Chakraborty, S.; Kundu, S.P.; Basak, R.K.; Majumder, S.B.; Adhikari, B. Improvement in mechanical properties of jute fibers through mild alkali treatment as demonstrated by utilisation of the Weibull distribution model. *Bioresour. Technol.* **2012**, *107*, 222–228. [[CrossRef](#)] [[PubMed](#)]
63. Morton, W.E.; Hearle, J.W.S. Equilibrium Absorption of Water. In *Physical Properties of Textile Fibers*, 4th ed.; Morton, W.E., Hearle, J.W.S., Eds.; CRC Press: Cambridge, UK, 2008; pp. 178–194.
64. Baley, C.; Le Duigou, A.; Bourmaud, A.; Davies, P. Influence of drying on the mechanical behaviour of flax fibres and their unidirectional composites. *Compos. Part A Appl. Sci. Manuf.* **2012**, *43*, 1226–1233. [[CrossRef](#)]
65. Nam, S.; Netravali, A.N. Green composites. I. Physical properties of ramie fibers for environment-friendly green composites. *Fibers Polym.* **2006**, *7*, 372–379. [[CrossRef](#)]
66. Sgriccia, N.; Hawley, M.C.; Misra, M. Characterization of natural fiber surfaces and natural fiber composites. *Compos. Part A Appl. Sci. Manuf.* **2008**, *39*, 1632–1637. [[CrossRef](#)]
67. Joseph, P.V.; Joseph, K.; Thomas, S. Short sisal fiber reinforced polypropylene composites: The role of interface modification on ultimate properties. *Compos. Interfaces* **2002**, *9*, 171–205. [[CrossRef](#)]
68. Taj, S.; Munawar, M.A.; Khan, S. Natural fiber-reinforced polymer composites. *Proc. Pak. Acad. Sci.* **2007**, *44*, 129.
69. Alias, A.H.; Tahir, P.M.; Abdan, K.; Sapuan, M.S.; Wahab, M.S.; Saiman, M.P. Evaluation of kenaf yarn properties as affected by different linear densities for woven fabric laminated composite production. *Sains Malays.* **2018**, *47*, 1853–1860. [[CrossRef](#)]
70. Belaadi, A.; Bouchak, M.; Aouici, H. Mechanical properties of vegetal yarn: Statistical approach. *Compos. Part B Eng.* **2016**, *106*, 139–153. [[CrossRef](#)]
71. Xue, D.; Hu, H. Mechanical properties of biaxial weft-knitted flax composites. *Mater. Des.* **2013**, *46*, 264–269. [[CrossRef](#)]
72. Shukla, A.; Basak, S.; Ali, S.W.; Chattopadhyay, R. Development of fire retardant sisal yarn. *Cellulose* **2017**, *24*, 423–434. [[CrossRef](#)]